ChemComm

COMMUNICATION

View Article Online
View Journal | View Issue

Check for updates

Cite this: *Chem. Commun.*, 2024, **60**, 6431

Received 29th April 2024,
Accepted 28th May 2024

DOI: 10.1039/d4cc02065k

rsc.li/chemcomm

Open Access Article. Published on 28 May 2024. Downloaded on 5/22/2026 2:11:57 PM.
This article is licensed under a Creative Commons Attribution-NonCommercial 3.0 Unported Licence.

Mechanical bonding of rigid MORFs using a tetratopic rotaxane†

Adrian Saura-Sanmartin, [a] Guillermo Cutillas-Font, [a] Alberto Martinez-Cuezva, [a] Mateo Alajarin, [a] Fátima Esteban-Betegón, [b] Pilar Pena-Sánchez, [b] Felipe Gándara *[b] and Jose Berna *[a]

The preparation of highly rigid cobalt(II)- and copper(II)–organic frameworks incorporating a tetralactam [2]rotaxane as a ligand is described. The interlocked ligand is functionalized with two pairs of carboxylate groups placed at each counterpart, thus limiting its dynamics within the crystal. The solid structure of the metal–organic rotaxane frameworks showed different, unprecedented polycatenation modes of grids, depending on the employed metal, providing great rigidity to the structures. This rigidity has been evaluated by using single crystal X-ray diffraction analyses of the cobalt(II)–organic frameworks embedded in different solvents, observing that the lattices remain unchanged. Thus, this research demonstrates that rigid and robust materials with permanent porosity can be achieved using dynamic ligands.

The preparation of materials using mechanically interlocked molecules (MIMs) is a relevant research topic nowadays.[1] Indeed, this approach is postulated as a suitable strategy towards smart materials, among other advanced applications.[1,2] Rotaxanes, a class of MIMs having at least a macrocyclic component threaded by a linear one, have aroused great interest due to their higher versatility.[2] One of the focuses of the scientific community working in this area is the incorporation of these intertwined compounds into different materials.[1] In parallel, research on metal–organic frameworks (MOFs) has experienced exponential growth in the last decades,[3] mainly due to the wide range of functionalities achievable through diverse structural designs that combine metallic salts and organic ligands. Metal–organic rotaxane frameworks (MORFs) have rapidly emerged as a research subfield having great potential.[4] Thus, several examples of MORFs using various metals and a diversity of structurally different interlocked ligands have been reported.[5] Typically, MORFs incorporate mechanical bonds through rotaxane or pseudorotaxane linkers with carboxylic acid or pyridyl donors at the strut ends. By allowing the rotaxane rings to remain uncoordinated, the desired dynamism provided by the MIMs is imparted to the MOFs, even though the mechanical bond does not directly extend the network. Interestingly, the inherent dynamics of the rotaxane counterparts have been transferred from solution to the solid state by integrating them into the crystalline array of MORFs,[6] allowing advanced implementations such as mechanisorption.[6] Yaghi and Stoddart coined the term 'robust dynamics' to refer to the coupling of the dynamics of MIMs with the robust structures of MOFs.[7] Less commonly, rotaxanes including metal coordination sites both on the macrocycle and on the axle of the MIM-based linker are used.[8] In such cases, a rotaxane with coordination sites on both components can lead to novel catenation modes during the formation of extended structures through coordination with metal atoms.

Herein, the preparation of two novel MORFs having benzylic amide macrocycle-based ligands[9–11] is described.‡ In these materials, rotaxane **1** (see the ESI† for synthetic details) is employed as a tetratopic ligand (H4L) with metal-coordination sites both on the macrocycle and on the axle (Fig. 1a). Due to the significance of rigid MOFs,[12] the use of a rotaxane having four carboxylate groups, one pair placed at each interlocked counterpart, is envisioned for the first time as an alternative approach to alter the dimensionality of the framework material, alter the local and global dynamics and, thereby rigidify the target reticular materials. In contrast to the examples that seek to integrate the mechanical bonds to take advantage of the switchable motion in MOF pores, rotaxane **1** is used to provide two rigidity functions to the final crystalline array: (i) blocking the motion of the ligand counterparts, and (ii) introducing new network polycatenation modes. Although rotaxanes tend to be flexible molecules, the act of threading one molecule to another contributes to rigidifying the component molecules and, in this

[a] *Departamento de Química Orgánica, Facultad de Química, Regional Campus of International Excellence "Campus Mare Nostrum", Universidad de Murcia, 30100, Murcia, Spain. E-mail: ppberna@um.es*
[b] *Departamento de Nuevas Arquitecturas en Química de Materiales, Instituto de Ciencia de Materiales de Madrid (ICMM-CSIC), Sor Juana Inés de la Cruz 3, 28049, Madrid, Spain. E-mail: gandara@icmm.csic.es*

† Electronic supplementary information (ESI) available: Experimental procedures and characterization data. CCDC 2340441 and 2340442. For ESI and crystallographic data in CIF or other electronic format see DOI: https://doi.org/10.1039/d4cc02065k

Open Access Article. Published on 28 May 2024. Downloaded on 5/22/2026 2:11:57 PM.
This article is licensed under a Creative Commons Attribution-NonCommercial 3.0 Unported Licence.

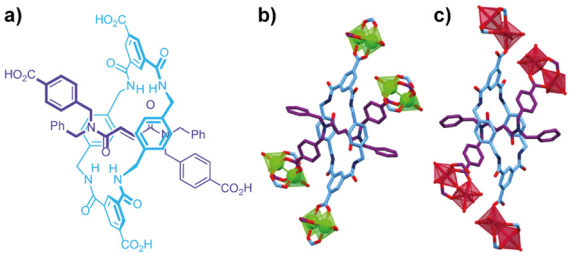

Fig. 1 (a) Chemical structure of the tetratopic rotaxane ligand **1**. Stick representation of a single unit of the rotaxane ligand coordinated to (b) four Cu(II) paddlewheel clusters of **UMUMOF-7** and (c) four Co(II) clusters of **UMUMOF-8**. Metals are shown in polyhedral representation (colored in green for copper and red for cobalt) and hydrogens are omitted.

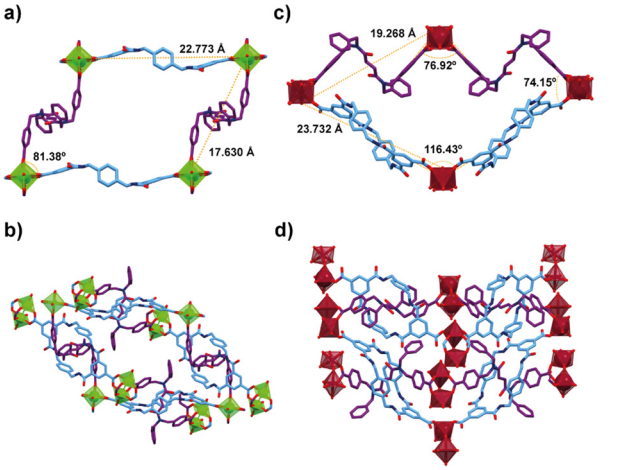

Fig. 2 (a) Stick representation of the rhombohedral metallogrid of **UMUMOF-7** having four copper(II) paddlewheels connected to four different ligands with one component of each rotaxane omitted. (b) The same grid showing all components. (c) Metallogrid of **UMUMOF-8** having four cobalt(II) nodes connected to four different ligands with one component of each rotaxane omitted. (d) The same grid showing all components.

way, they may make potentially rigid linkers[5,6] while offering certain conformational flexibility during the formation of the MOF backbone.

Rotaxane **1** was employed as the ligand in a solvothermal protocol (Fig. S1, ESI†)[8] which allows the preparation of the new MORFs. The Cu(II)-based MORF, so-called **UMUMOF-7**, $[Cu_2(H_2O)_2L]$, was obtained by reacting **1** with $Cu(NO_3)_2{\cdot}H_2O$, while in the Co(II)–organic framework, named **UMUMOF-8**, $[Co_2(H_2O)_5L]$, $Co(NO_3)_2{\cdot}6H_2O$ was employed as the metal source. **UMUMOF-7** was obtained as blue prismatic crystals in 64% yield (Fig. S2, ESI†), while reddish crystals of **UMUMOF-8** were collected in 60% yield (Fig. S3, ESI†). The IR spectrum of **UMUMOF-7** (Fig. S9, ESI†) shows a pair of carboxylate-copper symmetric and asymmetric stretching vibrations having values of 1331.13, 1357.64, 1593.88 and 1650.77 cm^{-1}, respectively. The corresponding carboxylate-cobalt signals of **UMUMOF-8** are shown at 1343.26, 1351.01, 1596.77 and 1649.80 cm^{-1} (Fig. S10, ESI†). The crystallinity of both materials was confirmed by X-ray powder diffraction measurements (Fig. S7 and S8, ESI†). Additionally, thermogravimetric analysis indicates a high thermal stability of **UMUMOF-7, -8** (Fig. S5, ESI†). Scanning electron microscopy micrographs reveal different morphologies for both materials, as well as a larger size in the case of the Co(II)-based crystals (Fig. S4, ESI†).

The elucidation of the periodic structures was successfully accomplished using single crystal X-ray diffraction (SCXRD), showing the crystallization of **UMUMOF-7** in the *C*2/*c* space group of the monoclinic crystal system. The repeating unit shows one rotaxane **1** connected to four symmetry related copper paddlewheel clusters through four carboxylate groups, two placed at the stoppers of the thread and two at the isophthalamide units of the macrocycle (Fig. 1b). A double bifurcated H-bond pattern is established between the counterparts of the interlocked ligand. The crystalline topology[13] disclosed the formation of 2D-rhombohedral metallogrids that connect four copper(II) paddlewheel clusters to four different organic ligands by propagating the repeating unit (Fig. 2a). The four-connected inorganic secondary building unit (SBU) is coordinated with two macrocycles and two threads, forming two-periodic square lattice (**sql**) layers. In these layers, the macrocycles and threads are alternately arranged around the square-shaped inorganic SBUs resulting in grids with dimensions of 22.77 × 17.63 $Å^2$ (SBU-to-SBU distance). Polycatenation between these coordinatively extended **sql** layers through their arrangement creates a three-dimensional structure, facilitated by the rotaxane linkers. The specific arrangement of macrocycles and threads around the SBUs leads to a polythreading interaction between the coordination layers, where each layer contributes both rings and rods to the mechanical interlocking (Fig. 3a and c).

UMUMOF-8 crystallizes in the *Pnma* space group of the orthorhombic crystal system. The inorganic SBU is also diatomic, with cobalt atoms in an octahedral environment (Fig. 1b). This structure also includes four carboxylic groups, contributing to a four-connected SBU configuration that facilitates the development of **sql** layers, although these layers exhibit more pronounced distortion from the ideal square arrangement. In this arrangement, the distances of the grid are 23.73 × 19.27 $Å^2$. Notably, the arrangement of macrocycles and linear connecting elements around the SBU differs in this case; two adjacent macrocycles are paired together, as are two linear elements. This disposition of cycles and rods around the SBU leads to a unique polycatenation pattern among the layers. Specifically, the interlayer threading process is characterized by an alternating contribution from each layer: one layer provides the macrocycles, while the adjacent layer supplies the linear elements (Fig. 3b and d).

As in the copper(II)-based material, the other components of the ligands, which are not involved in the formation of the 2D-metallogrid, extend the dimensionality of the crystalline array (Fig. 2d). The metallogrids of **UMUMOF-7, -8** are repeatedly extended along the directions of threads and macrocycles, observing parallel lines of threads and macrocycles in **UMUMOF-7** (Fig. S13a, ESI†) and a waving disposition in **UMUMOF-8** (Fig. S13b, ESI†). The 3D growth of both materials provides highly interconnected frameworks. Compared to other

 This journal is © The Royal Society of Chemistry 2024

Open Access Article. Published on 28 May 2024. Downloaded on 5/22/2026 2:11:57 PM.
This article is licensed under a Creative Commons Attribution-NonCommercial 3.0 Unported Licence.

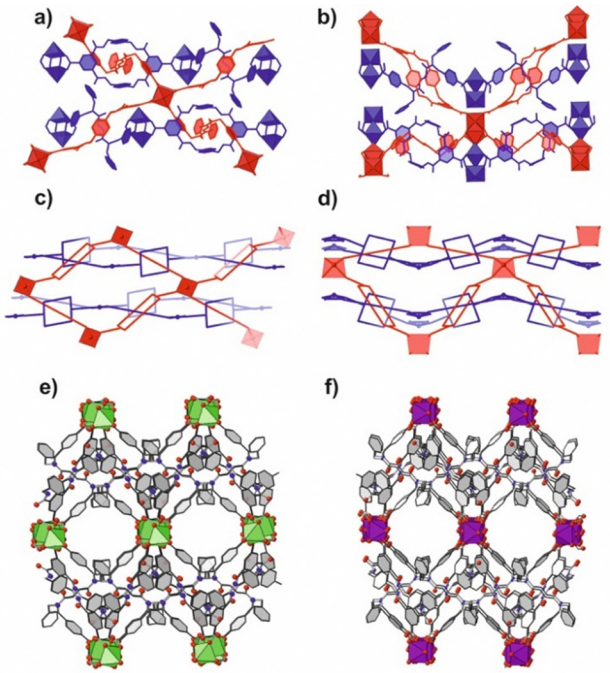

Fig. 3 Polyhedral and stick representation of the catenation modes in **UMUMOF-7** (a) and **UMUMOF-8** (b). Catenation takes place between layers with different colors (blue and red). Simplified views are shown in (c) and (d), where the inorganic SBUs are simplified as solid squares, and the linkers are simplified as cycles and rods. Polyhedral and ball and stick display of the structure of **UMUMOF-7** (e) and **UMUMOF-8** (f), showing the generated channels running along the *c* and *b* axes, respectively.

examples of MOFs using tetralactam macrocycles as ligands, the structures reported herein offer unique structural properties. Indeed, while the employment of related macrocycles as ligands led to 1D frameworks having big pores[10] and the use of an analogous rotaxane having only coordination groups placed at the macrocycle component allowed the formation of 2D networks,[9] these novel examples showed a 3D polycatenated structure through the polythreading of the linkers. Thus, a new approach to control dimensionality is established, not only by just selecting between a non-interlocked or an interlocked related ligand, but also by the rational positioning of the coordination elements, either exclusively on one component or both counterparts of the rotaxane ligand, which ensures the presence of mechanical bonding between coordination layers.

Therefore, the analysis of the crystalline structures indicates that the rational design of ligand **1** leads to the obtention of the envisioned requirements, since both rotaxane counterparts are connected to different clusters in a robust matrix and a three-dimensional arrangement that facilitates polycatenation is obtained. Thus, the final 3D structures having high density of interconnected metallogrids suggest highly rigid frameworks. A detailed analysis of the SCXRD structures considering the rhombohedral metallogrids as repeating units revealed a concatenation through the mechanical bond of rotaxane **1**, since these grids are extended in all dimensions through the different counterparts of the interlocked ligand (Fig. 3a and b). These concatenated grids are likely responsible for the great stiffness of the lattices. The impeded motion of macrocycles and threads in the rotaxane linkers as a consequence of their full integration into the crystalline array should avoid the flexibility that characterizes other MOFs incorporating interlocked ligands with tetralactam macrocycles.[9,11] Despite this 3D arrangement of ligands within the frameworks, which rigidify the target materials, the disposition of the grids forms channels that allow the uptake of small molecules. Channels along the *c* axis are formed within the solid structure of **UMUMOF-7** (Fig. 3e), having a calculated solvent-accessible volume of 28.9% of the total volume (2179.0 Å^3).[14] This value decreases to 2184.2.0 Å^3 (27.5% of the total volume) in **UMUMOF-8**, forming channels along the *b* axis (Fig. 3f). CO_2 adsorption experiments indicate a higher pore surface area in the cobalt(II)–organic framework, albeit with similar pore volume values (Table S1, ESI†).

With the aim of confirming experimentally the great rigidity suggested by the solid structure of the frameworks, an experiment using different solvents was designed. Analogous experiments using **MIL-53(Fe)** have determined alterations in the framework structure that affects the breathing phenomenom,[15] even observing changes in space groups when the cell volume increases due to the solvent employed. The test reported herein involves the evacuation of the solvent by washing crystals of **UMUMOF-8** with ethanol, followed by drying under vacuum. The obtained crystals were embedded in three different solvents of various polarity (ethanol, toluene or bromobenzene) to evaluate possible structural changes in the MOFs. SCXRD measurements were subsequently conducted, and the main crystallographic data for each one of the collected crystals are given in ESI† Tables S2–S4. In all cases, no significant changes were observed in cell volumes or crystal symmetry, demonstrating the high robustness and rigidity of the materials. The position of the adsorbed solvent molecules was clearly visible in the refined structures, with areas of high electron density in the pores. The location of the solvent molecules in the pores (Fig. S14–S17, ESI†) demonstrates their interaction with the framework atom, and their particular arrangement. Thus, toluene and bromobenzene molecules are found forming van der Waals interactions with the pendant phenyl rings of the linkers (Fig. 4), which do not show any deviation from their original conformation. In the case of ethanol molecules, they are found to form hydrogen bonds with the inorganic SBUs, but the framework atoms are not altered (see Table S4, ESI†), and the overall polycatenated structure remains unaffected. The data obtained in this study confirm that the use of a tetratopic rotaxane ligand and the resulting polythreading pattern result in a highly rigid MOF, affording a very robust material. Interestingly, in contrast to the elasticity provided by the tetratopic catenane ligands employed by Sato and colleagues,[11] the employment of a tetratopic rotaxane leads to the target rigidity.

In summary, a novel synthetic approach towards rigid metal–organic frameworks from a flexible ligand, which in this case is a [2]rotaxane, has been developed. A rational design that involves the increase of the number of carboxylate units of the interlocked ligand, *i.e.* two pairs placed one at the macrocycle and the other at the thread respectively, leads to the

Open Access Article. Published on 28 May 2024. Downloaded on 5/22/2026 2:11:57 PM.
This article is licensed under a Creative Commons Attribution-NonCommercial 3.0 Unported Licence.

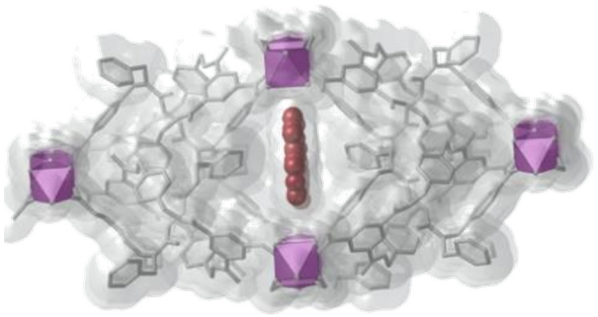

Fig. 4 Representation of the van der Waals interaction between **UMUMOF-8** and adsorbed toluene atoms (represented as red balls).

augmentation of the dimensionality and concatenation of the lattices of the framework, through a novel polycatenation mode, which provide the materials with high rigidity and robustness. Thus, the interlocked structure remains unchanged even when different solvents are employed. In this way, the morphology of the pores and, consequently, of the channels is retained constant, which allows applications that require an invariable pore size.

This work was supported by the MICIN/AEI/10.13039/501100011033 (Project PID2020-113686GB-I00, PID2021-123287OB-I00) and Fundacion Seneca-CARM (Project 21907/PI/22). G. Cutillas-Font thanks Fundacion Seneca-CARM for his contract (21442/FPI/20). A. Saura-Sanmartin thanks Ministerio de Universidades of the Government of Spain for his Margarita Salas postdoctoral contract (financed by the European Union – NextGenerationEU).

Conflicts of interest

There are no conflicts to declare.

Notes and references

‡ CCDC 2340441 and 2340442 contain the supplementary crystallographic data of the metal–organic materials **UMUMOF-7** and **UMUMOF-8**, respectively.

1 S. Mena-Hernando and E. M. Pérez, *Chem. Soc. Rev.*, 2019, **48**, 5016–5032.
2 M. Xue, Y. Yang, X. Chi, X. Yan and F. Huang, *Chem. Rev.*, 2015, **115**, 7398–7501.
3 (*a*) N. W. Ockwig, O. Delgado-Friedrichs, M. O'Keeffe and O. M. Yaghi, *Acc. Chem. Res.*, 2005, **38**, 176–182; (*b*) M. O'Keeffe, M. A. Peskov, S. J. Ramsden and O. M. Yaghi, *Acc. Chem. Res.*, 2008, **41**, 1782–1789; (*c*) A. Schneemann, V. Bon, I. Schwedler, I. Senkovska, S. Kaskel and R. A. Fischer, *Chem. Soc. Rev.*, 2014, **43**, 6062–6096; (*d*) R. Freund, S. Canossa, S. M. Cohen, W. Yan, H. Deng, V. Guillerm, M. Eddaoudi, D. G. Madden, D. Fairen-Jimenez, H. Lyu, L. K. Macreadie, Z. Ji, Y. Zhang, B. Wang, F. Haase, C. Wöll, O. Zaremba, J. Andreo, S. Wuttke and C. S. Diercks, *Angew. Chem., Int. Ed.*, 2021, **60**, 23946–23974; (*e*) R. Freund, O. Zaremba, G. Arnauts, R. Ameloot, G. Skorupskii, M. Dincă, A. Bavykina, J. Gascon, A. Ejsmont, J. Goscianska, M. Kalmutzki, U. Lächelt, E. Ploetz, C. Diercks and S. Wuttke, *Angew. Chem., Int. Ed.*, 2021, **60**, 23975–24001; (*f*) S. J. Lee and S. G. Telfer, *Angew. Chem., Int. Ed.*, 2023, **62**, e202306341.
4 (*a*) V. N. Vukotic and S. J. Loeb, *Chem. Soc. Rev.*, 2012, **41**, 5896–5906; (*b*) B. H. Wilson and S. J. Loeb, *Chem*, 2020, **6**, 1604–1612; (*c*) A. Saura-Sanmartin, A. Pastor, A. Martinez-Cuezva, G. Cutillas-Font, M. Alajarin and J. Berna, *Chem. Soc. Rev.*, 2022, **51**, 4949–4976.
5 (*a*) D. Whang, Y.-M. Jeon, J. Heo and K. Kim, *J. Am. Chem. Soc.*, 1996, **118**, 11333–11334; (*b*) D. Whang and K. Kim, *J. Am. Chem. Soc.*, 1997, **119**, 451–452; (*c*) E. Lee, J. Heo and K. Kim, *Angew. Chem., Int. Ed.*, 2000, **39**, 2699–2701; (*d*) G. J. E. Davidson and S. J. Loeb, *Angew. Chem., Int. Ed.*, 2003, **42**, 74–77; (*e*) D. J. Hoffart and S. J. Loeb, *Angew. Chem., Int. Ed.*, 2005, **44**, 901–904; (*f*) S. J. Loeb, *Chem. Commun.*, 2005, 1511–1518; (*g*) X.-D. Zhang, Y. Zhao, K. Chen, X.-Y. Dao, Y.-S. Kang, Y. Liu and W.-Y. Sun, *Chem. – Eur. J.*, 2020, **26**, 2154–2158; (*h*) H. Ju, M. Shin, I.-H. Park, J. H. Jung, J. J. Vittal and S. S. Lee, *Inorg. Chem.*, 2021, **60**, 8285–8292; (*i*) X. Li, J. Xie, Z. Du, R. Yu, J. Jia, Z. Chen and K. Zhu, *Chem. Commun.*, 2022, **58**, 5829–5832; (*j*) J. Geng, L. Mei, Y. Liang, L. Yuan, J. Yu, K. Hu, L. Yuan, W. Feng, Z. Chai and W. Shi, *Nat. Commun.*, 2022, **13**, 2030; (*k*) X. Li, Z. Du, L. Jiang, S. Ling and K. Zhu, *Chem. Sci.*, 2022, **13**, 6291–6296.
6 (*a*) V. N. Vukotic, K. J. Harris, K. Zhu, R. W. Schurko and S. J. Loeb, *Nat. Chem.*, 2012, **4**, 456–460; (*b*) K. Zhu, V. N. Vukotic, C. A. O'Keefe, R. W. Schurko and S. J. Loeb, *J. Am. Chem. Soc.*, 2014, **136**, 7403–7409; (*c*) V. N. Vukotic, C. A. O'Keefe, K. Zhu, K. J. Harris, C. To, R. W. Schurko and S. J. Loeb, *J. Am. Chem. Soc.*, 2015, **137**, 9643–9651; (*d*) K. Zhu, C. A. O'Keefe, V. N. Vukotic, R. W. Schurko and S. J. Loeb, *Nat. Chem.*, 2015, **7**, 514–519; (*e*) P. R. McGonigal, P. Deria, I. Hod, P. Z. Moghadam, A.-J. Avestro, N. E. Horwitz, I. C. Gibbs-Hall, A. K. Blackburn, D. Chen, Y. Y. Botros, M. R. Wasielewski, R. Q. Snurr, J. T. Hupp, O. K. Farha and J. F. Stoddart, *Proc. Natl. Acad. Sci. U. S. A.*, 2015, **112**, 11161–11168; (*f*) B. H. Wilson, C. S. Vojvodin, G. Gholami, L. M. Abdulla, C. A. O'Keefe, R. W. Schurko and S. J. Loeb, *Chem*, 2020, **7**, 202–211; (*g*) L. Feng, Y. Qiu, Q.-H. Guo, Z. Chen, J. S. W. Seale, K. He, H. Wu, Y. Feng, O. K. Farha, R. D. Astumian and J. F. Stoddart, *Science*, 2021, **374**, 1215–1221; (*h*) B. H. Wilson, L. M. Abdulla, R. W. Schurko and S. J. Loeb, *Chem. Sci.*, 2021, **12**, 3944–3951; (*i*) G. Gholami, B. H. Wilson, K. Zhu, C. A. O'Keefe, R. W. Schurko and S. J. Loeb, *Faraday Discuss.*, 2021, **225**, 358–370.
7 H. Deng, M. A. Olson, J. F. Stoddart and O. M. Yaghi, *Nat. Chem.*, 2010, **2**, 439–443.
8 (*a*) N. C. Frank, D. J. Mercer and S. J. Loeb, *Chem. – Eur. J.*, 2013, **19**, 14076–14080; (*b*) G. Gholami, K. Zhu, J. S. Ward, P. E. Kruger and S. J. Loeb, *Eur. J. Inorg. Chem.*, 2016, 4524–4529; (*c*) G. Gholami, G. Baggi, K. Zhu and S. J. Loeb, *Dalton Trans.*, 2017, **46**, 2462–2470.
9 A. Saura-Sanmartin, A. Martinez-Cuezva, D. Bautista, M. R. B. Marzari, M. A. P. Martins, M. Alajarin and J. Berna, *J. Am. Chem. Soc.*, 2020, **142**, 13442–13449.
10 A. Saura-Sanmartin, A. Martinez-Cuezva, M. Marin-Luna, D. Bautista and J. Berna, *Angew. Chem., Int. Ed.*, 2021, **60**, 10814–10819.
11 W. Meng, S. Kondo, T. Ito, K. Komatsu, J. Pirillo, Y. Hijikata, Y. Ikuhara, T. Aida and H. Sato, *Nature*, 2021, **598**, 298–303.
12 (*a*) N. B. Shustova, A. F. Cozzolino and M. Dincă, *J. Am. Chem. Soc.*, 2012, **134**, 19596–19599; (*b*) R.-B. Lin, L. Li, H.-L. Zhou, H. Wu, C. He, S. Li, R. Krishna, J. Li, W. Zhou and B. Chen, *Nat. Mater.*, 2018, **17**, 1128–1133; (*c*) Z. Chen, P. Li, X. Zhang, P. Li, M. C. Wasson, T. Islamoglu, J. F. Stoddart and O. K. Farha, *J. Am. Chem. Soc.*, 2019, **141**, 2900–2905; (*d*) R. Lyndon, Y. Wang, I. M. Walton, Y. Ma, Y. Liu, Z. Yu, G. Zhu, S. Berens, Y.-S. Chen, S. G. Wang, S. Vasenkov, D. S. Sholl, K. S. Walton, S. H. Pang and R. P. Lively, *Chem. Commun.*, 2022, **58**, 12305–12308; (*e*) Y. Xiao, Y. Chen, W. Wang, H. Yang, A. N. Hong, X. Bu and P. Feng, *J. Am. Chem. Soc.*, 2023, **145**, 10980–10986.
13 (*a*) D. Kim, X. Liu and M. S. Lah, *Inorg. Chem. Front.*, 2015, **2**, 336–360; (*b*) A. Schoedel, M. Li, D. Li, M. O'Keeffe and O. M. Yaghi, *Chem. Rev.*, 2016, **116**, 12466–12535; (*c*) G. C. Lisensky and O. M. Yaghi, *J. Chem. Educ.*, 2022, **99**, 1998–2004.
14 P. van der Sluis and A. L. Spek, The values of the solvent-accessible volume were calculated with the PLATON SQUEEZE program, *Acta Crystallogr., Sect. A: Found. Crystallogr.*, 1990, **46**, 194–201.
15 F. Millange, C. Serre, N. Guillou, G. Férey and R. I. Walton, *Angew. Chem., Int. Ed.*, 2008, **47**, 4100–4105.

 This journal is © The Royal Society of Chemistry 2024